Characteristics of a tunneling quantum-dot infrared photodetector operating at room temperature

P. Bhattacharya,[a] X. H. Su, and S. Chakrabarti
Solid State Electronics Laboratory, Department of Electrical Engineering and Computer Science,
University of Michigan, Ann Arbor, Michigan 48109-2122

G. Ariyawansa and A. G. U. Perera
Department of Physics and Astronomy, Georgia State University, Atlanta, Georgia 30303

We report high-temperature (240–300 K) operation of a tunneling quantum-dot infrared photodetector. The device displays two-color characteristics with photoresponse peaks at ~6 μm and 17 μm. The extremely low dark current density of 1.55 A/cm^2 at 300 K for 1 V bias is made possible by the tunnel filter. For the 17 μm absorption, the measured peak responsivity is 0.16 A/W (300 K) for a bias of 2 V and the specific detectivity D^* is 1.5×10^7 cm Hz$^{1/2}$/W (280 K) for a bias of 1 V. Excellent performance characteristics are also measured for the 6 μm photoresponse. © *2005 American Institute of Physics*. [DOI: 10.1063/1.1923766]

A significant reduction in the cost of an infrared camera is possible if the traditional cooling systems with liquid nitrogen are replaced by thermoelectric coolers, or the array can be operated at room temperature. There is, therefore, an urgency to develop infrared photodetectors that operate at elevated temperatures. The quantum-dot infrared photodetector (QDIP)[1–3] has emerged as an interesting, and potentially viable device, wherein three-dimentional quantum confinement promises low dark currents, leading to a large detectivity. Additionally, in these devices, polarization selection rules allow absorption of normally incident light and the long effective carrier lifetime ~100's of picoseconds, confirmed by theory[4] and experiments,[5] provides the potential for large responsivity. Rapid progress has been made in the development of these devices and recently reported performance characteristics[6–11] (low dark currents, peak responsivity $\geqslant$0.5 A/W and specific detectivity $\sim10^{10}$–10^{11} cm Hz$^{1/2}$/W in the temperature range $\sim$80–150 K) are cause for optimism.

Unlike those in bulk *p-n* junction detectors or in quantum-well infrared photodetectors, the density of states of the self-organized In(Ga)As/GaAs quantum dots in QDIPs is represented by broadened δ-functions for the electron and hole ground and excited states. Even though the density of states is discrete for low-energy states, it tends to become like three-dimensional continuous states at high energies. As a result, at temperatures above ~150 K, the electron occupation is dominated by the excited states. Therefore, in the conventional QDIP, dark current benefits are difficult to sustain at temperatures above 150 K. *The reduction of dark current at high temperatures of operation is one of the biggest challenges in the design of QDIPs*. The problem stems from the commonality of the transport paths of carriers contributing to the dark- and photocurrent. Hence, any heterostructure design aimed at reducing the dark current also reduces the photocurrent and responsivity. We have recently reported the properties of a device—the tunneling QDIP (Ref. 12)—in which the electrons contributing to the photocurrent are selectively collected from the quantum dots

by resonant tunneling, while these same tunnel barriers block the electrons, with a broad energy distribution, that contribute to the dark current. We have shown theoretically and experimentally, a reduction of dark current by two orders of magnitude in tunneling QDIPs.[12] In this letter, we demonstrate room temperature operation of tunneling QDIPs, with a slightly modified design, with response peaks at wavelengths of ~6 μm and 17 μm.

The band diagram of the tunneling QDIP (T-QDIP) under an applied transverse bias is shown in Fig. 1(a). The double-barrier resonant tunneling heterostructure serves to decouple the dark- and photocurrent. The purpose of the single Al$_{0.1}$Ga$_{0.9}$As barrier, asymmetrically placed on the side of the dot opposite to the tunnel barriers, is to create well-defined quasi-bound final states in the quantum well for the photoexcited electrons. These states are also made to resonate with the tunneling states in the In$_{0.1}$Ga$_{0.9}$As/Al$_{0.3}$Ga$_{0.7}$As double barrier heterostructure. The tunnel probability is therefore near unity, as confirmed by calculations, for photoexcited electron transitions whose energies coincide with the QD bound state-to-well final state energy difference. The incorporation of the Al$_{0.1}$Ga$_{0.9}$As barrier also allows slight tuning of the peak response wavelength without having to change the quantum dot heterostructure design or the growth parameters. By simply adjusting the separation of the Al$_{0.1}$Ga$_{0.9}$As barrier from the quantum dot, the energy position of the quasi-bound state in the well can be tuned. The bound state energies in the quantum dot, as indicated in Fig. 1(a), were calculated by an eight-band $\mathbf{k} \cdot \mathbf{p}$ model[13] and the energy level in the quantum well is calculated by solving the one-dimensional Schrödinger equation including the presence of the wetting layer. The complete device heterostructure, grown by molecular-beam epitaxy, is schematically illustrated in Fig. 1(b). The GaAs and AlGaAs layers were grown at 610 °C and the quantum dot layers were grown at 500 °C. Mesa-shaped vertical devices for top illumination were fabricated by standard photolithography, wet chemical etching, and contact metallization techniques. The *n*-type top ring contact and the bottom contact were formed by evaporated Ni/Ge/Au/Ti/Au=250/325/650/200/2000 Å. The radius

a)Electronic mail: pkb@eecs.umich.edu
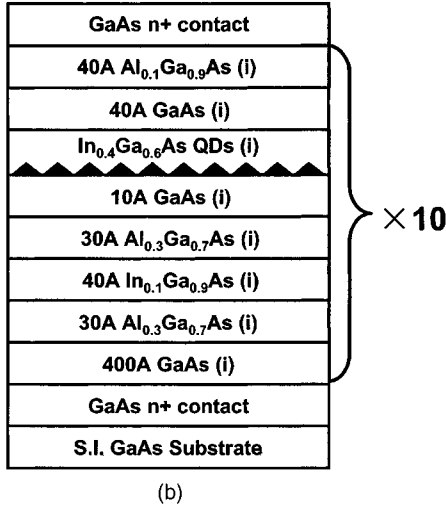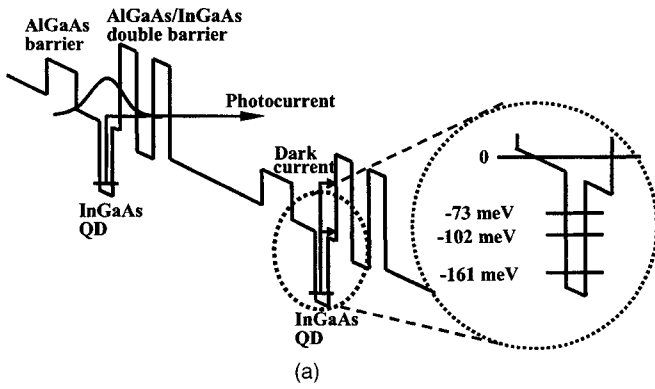
86, 191106-1

(a)

(b)

FIG. 1. (a) Schematic diagram of the conduction band profile of the T-QDIP under an applied transverse bias along with the calculated bound state energies in the dots and wells. (b) Schematic heterostructure of a T-QDIP grown by molecular-beam epitaxy.

of the illuminated area varies from $100-300$ μm. For testing purpose, devices are mounted onto chip carriers with silver epoxy and then bonded to the carrier leads using gold wire. The chip carrier is inserted into a liquid-helium cryostat for low-temperature measurements.

While the devices have been characterized in all the wavelength ranges of interest, in this letter, we mainly focus on their long wavelength detection characteristics at high temperatures. The dark current-voltage characteristics in the temperature range $240-300$ K, measured with a HP 4145 Semiconductor Parameter Analyzer, are shown in Fig. 2. The dark currents are substantially lower than those measured in
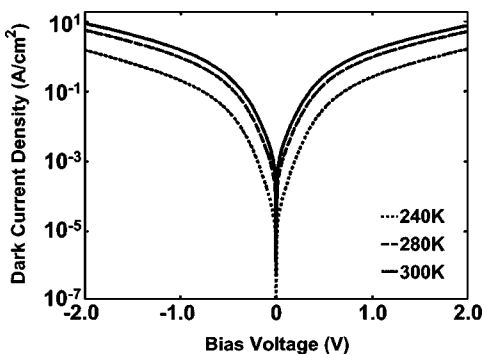

FIG. 2. Measured dark current density as a function of bias in the temperature range $240-300$ K.
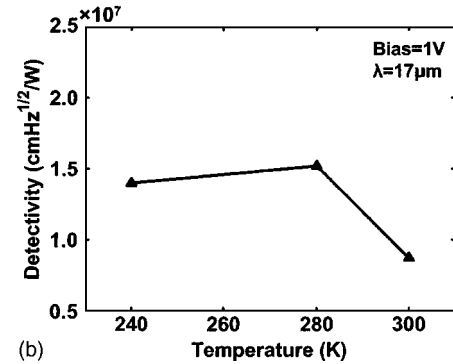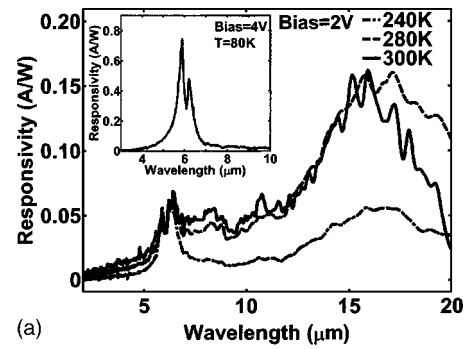

(a)

(b)

FIG. 3. (a) Measured spectral responsivity of T-QDIP in the temperature range $240-300$ K under a 2 V bias. The inset shows spectral responsivity at 80 K under a bias of 4 V. (b) Peak detectivity as a function of temperature for the 17 μm response derived from noise spectra measurements.

identical QDIPs without the tunneling double barriers. As stated earlier, we have reported[12] a measured and calculated reduction by nearly two orders of magnitude. From the data of Fig. 2, the values of J_{dark} at a bias of 1 V are 0.21, 0.96, and 1.55 A/cm^2 at 240, 280, and 300 K, respectively.

The spectral response and calibrated responsivity, under normal incidence, were measured with a globar broadband source ($1-20$ μm) and a BOMEM MB-155 Fourier transform infrared spectrophotometer. The spectral response of the QDIP under test and a composite bolometer with a known sensitivity are concurrently measured with the same combination of optical elements. Figure 3(a) shows the spectral response measured with an applied bias of 2 V in the temperature range $240-300$ K. There are two distinct absorption peaks, centered $\sim$6 μm and 17 μm and a weak response around 11 μm. On closer examination of the 6 μm transition, shown in the inset for measurement at 80 K with 4 V bias, the spectral response exhibits closely spaced dual peaks with an energy separation of $\sim$15 meV. The dual peaks arise from coupling and splitting of the wave functions of the quantum-well states and the bound states of the double-barrier heterostructure and provide evidence of resonant tunneling in the operation of the device. The measured energy separation between the peaks agrees well with the calculated valued of 13.5 meV. Careful examination of the background absorption indicates that the dip between the peaks is not due to water and CO_2 absorption. By changing the bias, small redshifts have been observed for both the dual peaks and the dip between them. It may be noted that the peak responsivity is $\sim$0.75 A/W and the quantum efficiency is 16% for the 6 μm response at a bias of 4 V.

It is worthwhile to note that the long-wavelength (17 μm) absorption becomes significant at temperatures higher than 200 K and, as is evident from Fig. 3(a), its peak

responsivity, $\sim$0.16 A/W, at 300 K is even higher than that of the 6 μm peak. With reference to the calculated energies of the bound and quasi-bound states in the dot and well, shown in Fig. 1(a), it is apparent that the absorption peak at $\sim$6 μm results from transition of photoexcited electrons from the dot ground state to the quasi-bound state in the well ($\Delta E=161$ meV). The broad peak centered at 17 μm results from transitions from the second-excited state of the dot to the well state ($\Delta E=73$ meV). The width of the peak is due to the transition being in the long-wavelength infrared region. In fact, the transition linewidth is only $\sim$26 meV, which is remarkably close to the inhomogeneous broadening of the QD states at 300 K. We believe that the 17 μm transition is dominant at high temperatures because the probability of occupation of the dot excited states increases with temperature. Due to the symmetry of the dot geometry, the excited states have a higher degeneracy than the ground state. The degeneracy of the second excited states is 8,[13] while it is 2 for the ground state. Therefore, the total number of carriers in the excited states can be comparable to, or larger, than that in the ground state at high temperatures although the occupation probability is lower. Additionally, for the same incident power, there are more photons at 17 μm than at 6 μm. These characteristics help to explain a higher absorption peak at 17 μm compared to that at 6 μm for temperatures of 280 and 300 K. It may be noted that the weak transition at $\sim$11 μm corresponds almost exactly to the energy separation between the first-excited dot state and the well state ($\Delta E=102$ meV). The selection rules may account for the weak transition. The wave function of the first-excited dot states is antisymmetrical in space and the wave function of the final states in the well is almost symmetrical near the dot layer. These give rise to a small transition momentum matrix as well as low responsivity. In contrast, all initial and final states corresponding to the 6 μm and 17 μm transitions are symmetrical and the transitions are allowed. Finally, it is extremely important to note that it is the low dark current in the T-QDIP that makes detection possible at these high temperatures.

The QDIP photocurrent signal and noise are measured with a Keithley 428 Current Sensitive Amplifier and an Ono Sokki CF-360F fast Fourier transform (FFT) Analyzer, which displays an FFT spectrum of voltage versus frequency. A thick copper plate was used as a radiation block to provide the dark conditions for the measurement. The specific detectivity D^*, which is a measure of the signal-to-noise ratio of the device, was calculated from the noise density spectra and the peak responsivity. The values of D^* for the 17 μm response at a bias of 1 V are plotted in Fig. 3(b) as a function of temperature. The values of D^*, in the 10^7 cm Hz$^{1/2}$/W range, are reasonable at these high temperatures[14] and we are confident that with some redesigning of the device heterostructure, $D^* \sim 10^9$ cm Hz$^{1/2}$/W can be demonstrated at room temperature. The measured D^* for the 6 μm absorption peak is 2.4×10^{10} cm Hz$^{1/2}$/W for a bias of 2 V at 80 K.

In conclusion, we report the characteristics of a two-color tunneling QDIP at high temperatures. 300 K operation is made possible by the incorporation of a double-barrier tunnel filter, which reduced the dark current to very low levels.

[1] J. Phillips, K. Kamath, and P. Bhattacharya, Appl. Phys. Lett. **72**, 2020 (1998).

[2] S. Maimon, E. Finkman, and G. Bahir, Appl. Phys. Lett. **73**, 2003 (1998).

[3] D. Pan, E. Towe, and S. Kennerly, Appl. Phys. Lett. **73**, 1937 (1998).

[4] B. Kochman, A. D. Stiff-Roberts, S. Chakrabarti, J. D. Phillips, S. Krishna, J. Singh, and P. Bhattacharya, IEEE J. Quantum Electron. **39**, 459 (2003).

[5] J. Urayama, T. B. Norris, J. Singh, and P. Bhattacharya, Phys. Rev. Lett. **86**, 4930 (2001).

[6] E. Kim, A. Madhukar, Z. Ye, and J. C. Campbell, Appl. Phys. Lett. **84**, 3277 (2004).

[7] S. Krishna, S. Raghavan, G. von Winckel, A. Stintz, G. Ariyawansa, S. G. Matsik, and A. G. U. Perera, Appl. Phys. Lett. **83**, 2745 (2003).

[8] S. Raghavan, P. Rotella, A. Stintz, B. Fuchs, S. Krishna, C. Morath, D. A. Cardimona, and S. W. Kennerly, Appl. Phys. Lett. **81**, 1369 (2002).

[9] L. Jiang, S. S. Li, N. T. Yeh, J. I. Chie, C. E. Ross, and K. S. Jones, Appl. Phys. Lett. **82**, 1986 (2003).

[10] S. Chakrabarti, A. D. Stiff-Roberts, P. Bhattacharya, S. D. Gunapala, S. Bandara, S. B. Rafol, and S. W. Kennerly, IEEE Photonics Technol. Lett. **16**, 1361 (2004).

[11] S. Chakrabarti, A. D. Stiff-Roberts, P. Bhattacharya, and S. W. Kennerly, Electron. Lett. **40**, 197 (2004).

[12] X. H. Su, S. Chakrabarti, A. D. Stiff-Roberts, J. Singh, and P. Bhattacharya, Electron. Lett. **40**, 1082 (2004).

[13] H. Jiang and J. Singh, Phys. Rev. B **56**, 4696 (1998).

[14] G. M. Williams and R. E. DeWames, J. Electron. Mater. **24**, 1239 (1995).